



Shallow water wave spectral characteristics in southwest Bay of Bengal using measurements from a moored buoy

Janakiram Reddy^{1,2} · Latha Ganesan¹ · Balamurugan Ramasubbu² · Venkatesan Ramasamy¹

Received: 1 March 2022 / Accepted: 22 April 2023 / Published online: 6 May 2023
© Saudi Society for Geosciences and Springer Nature Switzerland AG 2023

Abstract

Wave spectral characteristics are studied from the measurements made by a moored buoy off Chennai during 2017–2019. Time series wave data in shallow waters off Chennai have been obtained from a coastal buoy in the moored buoy network established and operated by the National Institute of Ocean Technology. Bay of Bengal (BoB) experiences three different weather conditions (i) pre-monsoon (February–May), (ii) South-west (SW)/summer monsoon (June–September), and (iii) North-east (NE)/post-monsoon (October–January). During the period between NE monsoon and SW monsoon (fair-weather), the coast experiences swell domination and, to an extent, wind sea driven and wave spectra are predominantly double peaked. During NE monsoon in November–December, it is a primarily single peaked and spectral peak period for fully developed wind sea equals peak wave period. Short period waves are dominated 65% of the time during the post-monsoon. The peak wave period ranges from 4 to 12 s for 81% of the time, and the predominant mean wave direction is between 135 and 180°. The significant wave height is less than 1.0 m for 61% of the time. The maximum wave height (H_{max}) observed is 4.0 m during cyclone Phethai. Two cyclones, Gaja and Phethai, were captured by the moored buoy, and wave spectra were analyzed during cyclone passage. The wave parameters of moored buoy are verified with measurements made by another buoy closely deployed, namely the PP WET buoy (Pilot Project on Wave Measurement, Evaluation and Testing (PP-WET) called PP WET buoy). The comparison shows that the correlation coefficient is 0.96 for significant wave height and 0.91 for the mean wave period for 2018. The comparison between the moored buoy and ERA5 significant wave heights during 2018 produces a higher correlation of 0.90, while the ERA5 data is overestimated by 33% during cyclone Phethai. The implications of this study would be helpful in wave data assimilation and operational forecasting in the coastal waters of the Bay of Bengal.

Keywords Wave characteristics · Wave spectra · Bay of Bengal · Moored buoy · Short period waves · PP WET buoy

Introduction

The ocean surface waves play a major role in the planning and design of coastal structures, navigation, and forecasting. Wave spectral energy density distributed over a range of frequencies is helpful to understand the wave climate of a particular region (Soares 1991; Hanson and Phillips 2001; Umesh et al. 2019a). Wind sea formed because of local wind

fields and swells propagating from far away carrying most of the energy at the sea surface (Semedo et al. 2011) can be distinguished from wave spectra (Johnson et al. 2012). Wave parameters are typically compared over different years to determine inter-annual variations in wave characteristics (Vanem and Walker 2013; Sanil Kumar and Anjali Nair 2015). The seasonal variations in winds generally reflect in wave climate; thus, it is important to analyze the spectral characteristics during different seasons (Kumar et al. 2014b).

Diurnal variations in wind speed and direction will affect the growth and decay of the wave spectrum (Nair et al. 2021). Due to the weak winds in April, the diurnal cycle caused by the sea breeze was visible along the west coast of India (Neetu et al. 2006). The sea breeze is active during the pre-monsoon season on the west coast of Goa (Aparna et al. 2005) and in the northwestern Bay of Bengal from October to January (Patra et al. 2016). In the southwestern BoB (off

Responsible Editor: Zhihua Zhang

✉ Janakiram Reddy
rjanakiram02@gmail.com

¹ National Institute of Ocean Technology, Ministry of Earth Sciences, Chennai, India

² Centre for Water Resources, Anna University, Chennai 600025, India

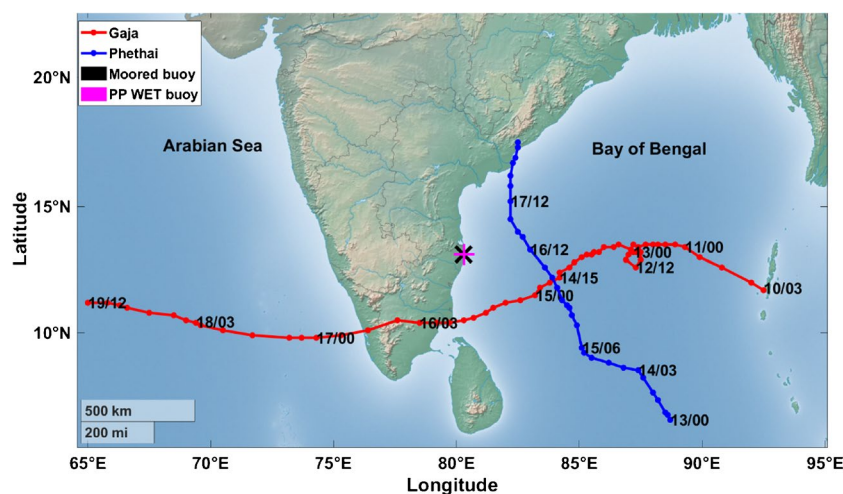
Puducherry), sea breeze causes an increase in wave height in the afternoon hours during SW monsoon, with a gradual decrease of its impact from June to September (Glejin et al. 2013). Similar, changes in wave height were observed during pre-monsoon (Glejin et al. 2013). During the SW monsoon (June to August), sea-breeze circulation was seen along the Chennai coast for 75% of the days and wind direction was from 140° (Simpson et al. 2007). On the east coast of India, sea breeze has been observed for May, and the direction of propagation is from south-east to southerly. The strength of the sea breeze is high on the west coast in comparison to the east coast of India (Srinivas et al. 2005). Hence sea breeze characteristics are not consistent on the east coast of India (Aboobacker et al. 2013).

Wave spectral characteristics along the eastern Arabian Sea show single peaked spectra during monsoon and double peaked spectra during the rest of the year. During monsoon, significant wave height of 4.2 m and maximum wave height of 7.0 m were observed (Kumar et al. 2014a). Aravind et al. 2021 studied monthly averaged wave spectra in the central west coast of India during 2015–2017 and found single peaked spectra during monsoon and multi peaked spectra were observed in March–April. Wave spectra are single peaked during October–November and double peaked spectra during the southwest monsoon in the northwestern BoB (Anjali et al. 2018). In general Bay of Bengal, the wave spectra are double or multi peaked spectra (Aboobacker et al. 2009). Wave spectra of southwestern BoB are multi peaked during SW monsoon and single peak spectra during post-monsoon (Glejin et al. 2013; Umesh et al. 2019a). Waves in northern BoB are rugged from June–Sept, May, and November–December (Kumar et al. 2014b), and the wave climate is influenced by both SW and NE monsoon (Kumar et al. 2004). SW monsoon, Southern Ocean swells, and cyclones influence the wave climate in the northwestern Bay of Bengal (Anjali et al. 2018). The southwestern Bay

of Bengal is a shadow area due to the south of Sri Lanka and the land area covered over the north a low energy state and wave height compared to the northern Bay of Bengal (Glejin et al. 2013). Hence, the influence of the SW monsoon is less in the present location, which is different from the west coast of India and north of BoB. The seasonal variations of measured spectra in coastal waters of the Bay of Bengal, studies have been carried out earlier by Kumar et al. 2014b; Patra et al. 2016; Glejin et al. 2013; Umesh et al. 2019a; Anjali et al. 2018; Umesh et al. 2019b. The east coast of India is characterized by a narrow continental shelf width as compared to the west coast (Aboobacker et al. 2009). Studies reported in this region using numerical models and measured wave spectrum for five months duration. The wave spectrum from a moored buoy off Chennai matches with the theoretical JONSWAP spectrum considering the wind conditions at sea (Vimala et al. 2014). Wave hindcast studies using WAVEWATCH III (Umesh and Behera 2020) and WAM cycle 4.5.3 (Swain et al. 2017) are performed in the north Indian Ocean. The derived wave parameters like significant wave height and mean wave period are validated with moored buoy data off Chennai. Extreme wave height analysis for different return periods was estimated for both significant wave height and maximum wave height off Chennai based on ERA-Interim data (Satish et al. 2019). Seasonal variations in the wave spectrum can be used to identify single, double, or multiple peaks in southwest BoB with varying sea states. Seasonal and annual variations in wave characteristics from in-situ measurements have not been studied earlier.

The tropical cyclones form in Bay of Bengal and the Arabian Sea are 5–6 in every year (Dube et al. 1997). Many studies were carried out in the past to understand wave characteristics during a cyclone (Kumar et al. 2004; Sanil Kumar et al. 2013; Jena et al. 2017; Sanil Kumar et al. 2014a; Glejin et al. 2013; Amrutha et al. 2014; Anjali et al. 2018; Nair

Fig. 1 The track of cyclones of Gaja and Phethai and location of buoy (map produced by MATLAB)



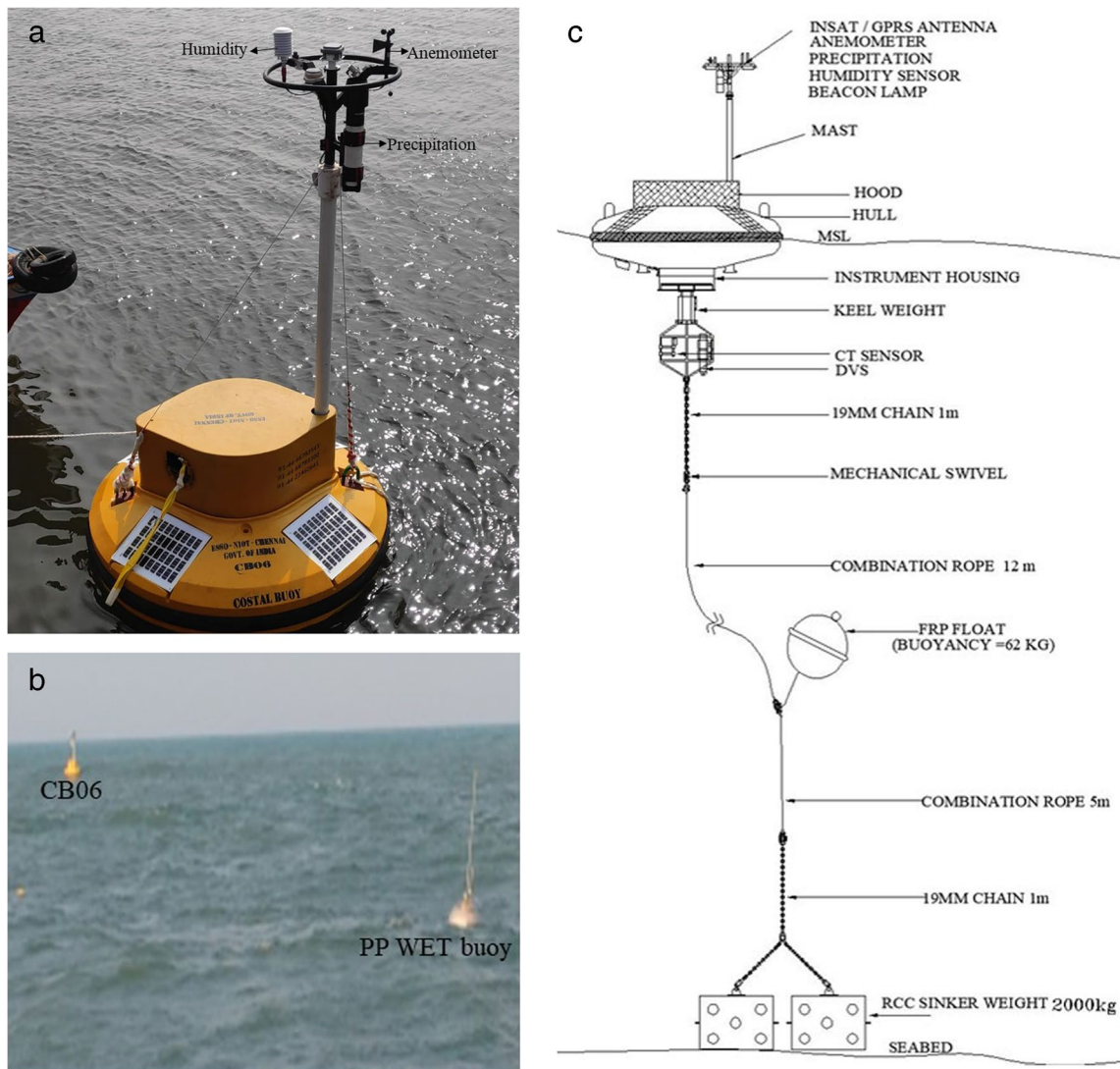


Fig. 2 Moored buoy of CB06 with meteorological sensors (a), closer view of CB06 and PP WET buoys (b) and buoy system of CB06 (c)

et al. 2021). Significant wave height increases and wave spectra are single peak during the cyclone period (Nair et al. 2021; Kumar et al. 2004). Maximum wave height up to 17.9 m were observed in northern BoB (21.00° N, 81.00° E) during the passage of tropical cyclone Aila (Kumar et al. 2020).

The present study focuses on Chennai. Such a study is very limited in the Bay of Bengal. The objective of this work is to study the wave spectral characteristics in the shallow waters of the southwest Bay of Bengal and their inter-annual variations using moored buoy time series observations. The effect of sea breeze on diurnal variations in local winds is also analyzed. In 2018, the wave spectrum features of the two cyclones Gaja and Phethai are analyzed. The observed wave characteristics from the moored buoy are compared with ERA5 reanalysis data and PP WET buoy data.

Materials and methods

Data

In situ observations of met-ocean parameters in the deep and shallow waters of the Arabian Sea and Bay of Bengal are made by a network of moored buoys deployed and maintained by the National Institute of Ocean Technology (NIOT), Chennai, under the Ministry of Earth Sciences, Government of India. Wave observations made in coastal southwestern BoB off Chennai, from 2017 to 2019, are used in this study. The measurements made by coastal moored buoy CB06

(13.1° N, 80.31° E) in shallow waters at a depth of 16m has been used (Fig. 1), which measures met-ocean parameters like wind, relative humidity, precipitation, air

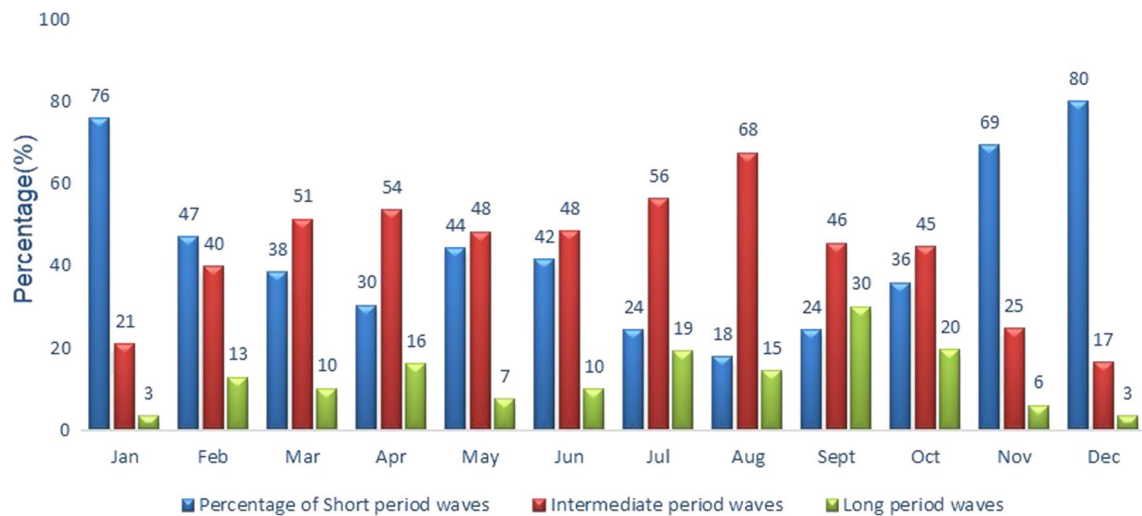


Fig. 3 Monthly percentage variations of short period waves, intermediate period waves and long period waves

temperature, sea level pressure, current speed and direction (1m depth of water), conductivity, and temperature (1 m depth of water). Motion Reference Unit (MRU) is used for measurement of waves (Fig. 2a and c). The primary sensors used in the MRU are accelerometers, angular rate sensors, and magnetometers. The Motion Reference Unit (SeaTex-MRU-6) sensor measures dynamic linear motion and altitude. The absolute roll, pitch, yaw (heading), and relative heave (dynamic) are the output of MRU recorded at a rate of 1 Hz for 17.06 minutes every 3 hours. Heave measured in a range from ± 50 m, period from 1 to 25 s and with dynamic accuracy of 5 cm or 5% whichever is highest. The high-frequency cut off was set at 0.5 Hz and the resolution was 0.001953 Hz. The raw data of absolute roll, pitch, heading, and relative heave are processed using MATLAB software which uses Fast Fourier Transform (FFT) on a wave record, and the wave spectrum is obtained.

The wind measurements are made by a cup/propeller type anemometer attached to the upper mast of the CB06 moored buoy (Fig. 2a). The data is recorded at 3 m above the sea level. The wind speed and direction are recorded every 3 h. The wind speeds from the moored buoy were transformed to wind speeds at 10 m elevations, using the Prandtl 1/7 law approximation (Sanil Kumar et al. 2010). The wind data of 2019 is used to study the sea and land breeze circulation.

The commonly used directional wave rider (DWR) is restricted to the coastal waters, which again limits the availability of wave data beyond coastal waters. The inception of the buoy network integrated with the Motion Reference Unit made it possible to measure the waves at any part of the ocean. The global community which mainly focuses on wave measurement using DWR, requested an inter-comparison with moored buoy, and intercomparison between wave data measured by moored buoy and DWR is carried out for the first time in Indian seas. This DWR buoy is called the PP

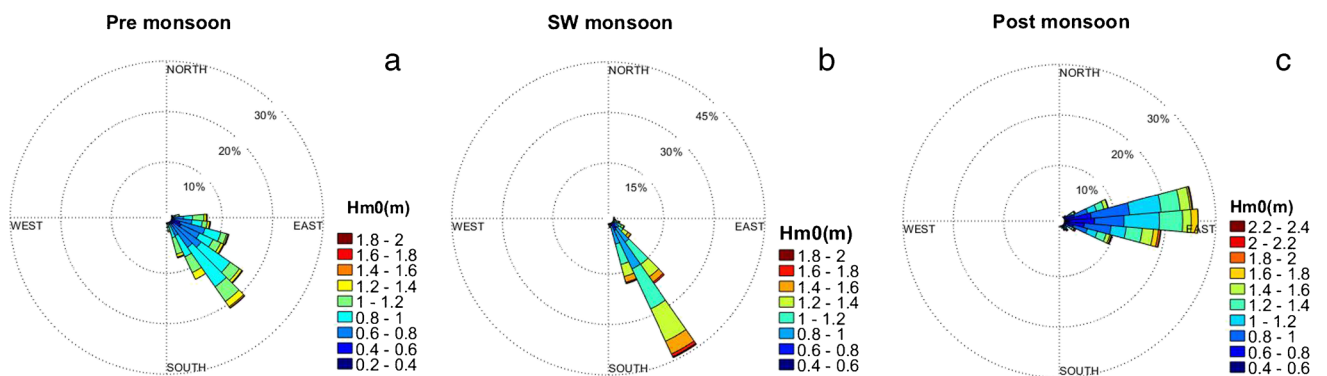


Fig. 4 Seasonal variation of wave direction short period waves during a pre-monsoon, b SW monsoon, and c post-monsoon

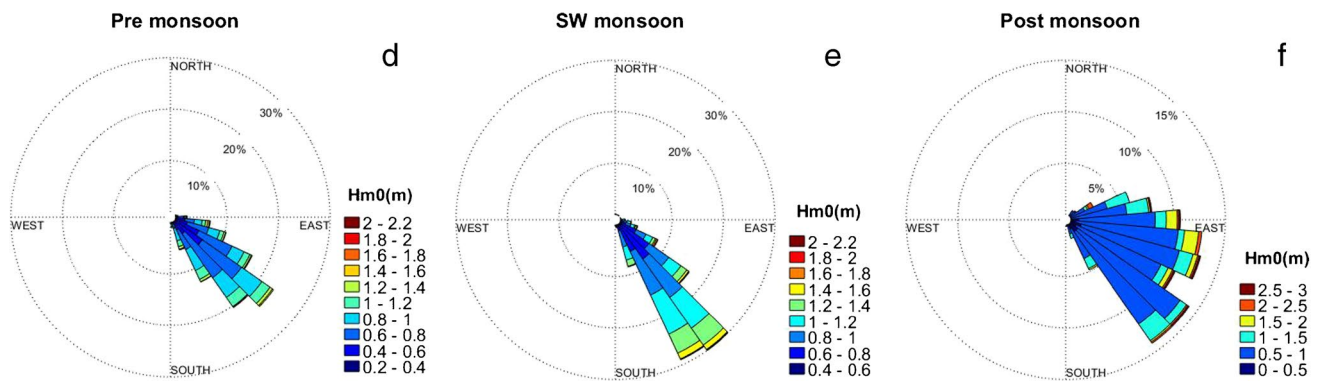


Fig. 5 Seasonal variation of wave direction intermediate period waves during **d** pre-monsoon, **e** SW monsoon, and **f** post-monsoon

WET buoy. The project aims to establish confidence in the user community of the validity of wave measurements from the various moored buoy systems. This project is supported by the joint WMO-IOC technical commission for oceanography and Marine Meteorology (JCOMM) and leading agencies such as Environment Canada, European services, Marine Observation program, and the National Oceanic and Atmospheric Administration (NOAA). Moored buoy (CB06) and DWR (13.1° N, 80.32° E) at 16 m water depth off Chennai deployed in February 2017 continued observations till 2019 for intercomparison of wave data as part of the JCOMM initiative. Both buoys are deployed at 1.0 km apart as shown in Fig. 2b. The data are recorded at a rate of 1.28 Hz for every 30 min. The internal memory data of Raw displacement data (.RDT) and Spectral data of one-month (.SDT) files are processed using Waves21 software. History of spectral parameters (.HIS) and Spectral data (.SPT) Ascii/Text files are obtained. Significant wave height and mean wave period data for 2017 to 2019 are obtained from these files and are used for intercomparing with CB06 moored buoy data.

ERA5 reanalysis data produced from European Centre for Medium-Range Weather Forecast (ECMWF) with a grid resolution of 0.5° X 0.5° at an interval of 3 hourly data utilized for the period 2017–2019. Significant wave height and mean wave period are obtained for the closest grid point of 13.0° N, 80.5° E (23 km from the moored buoy position) from the ERA5 data (<https://cds.climate.copernicus.eu/cdsapp#!/dataset/reanalysis-era5-single-levels?tab=form>). ERA5 data provides higher spatial and temporal resolution with an hourly estimate of data for the global atmosphere, land surface, and ocean waves (Hersbach et al. 2020). It offers data at a horizontal resolution of 31 km and with 137 levels in the vertical spanning from the surface up to 0.01 hPa. The past observations from the satellite are combined with the model data using the law of physics, the principle of data assimilation uses the latest version of the Integrated Forecasting System (IFS Cycle 41r2) to produce ERA5 data. The data is available from January 1, 1959, to near real-time. ERA5 is an open-source reanalysis long period data used for the study of various applications like wave climatology trends (Sreelakshmi and Bhaskaran 2020b; Muhammed Naseef and

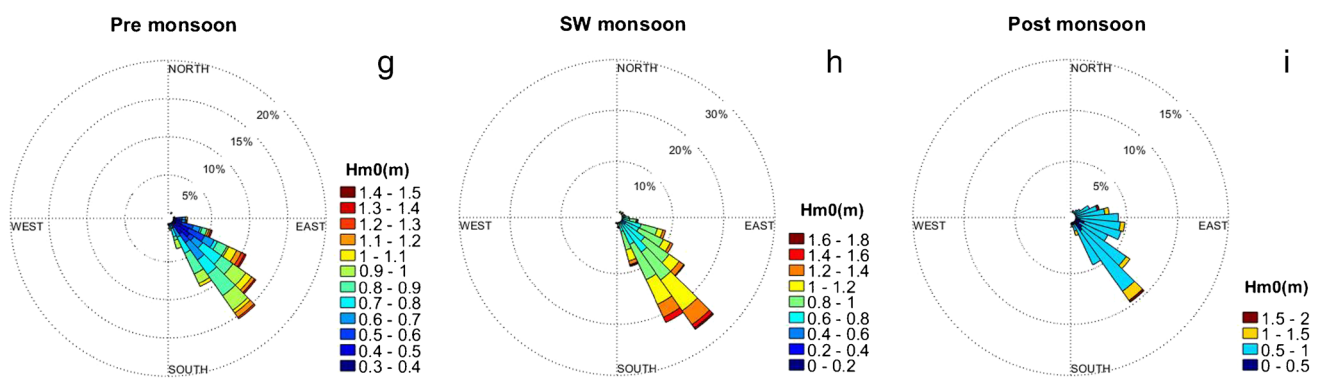


Fig. 6 Seasonal variation of wave direction long period waves during **g** pre-monsoon, **h** SW monsoon, and **i** post-monsoon

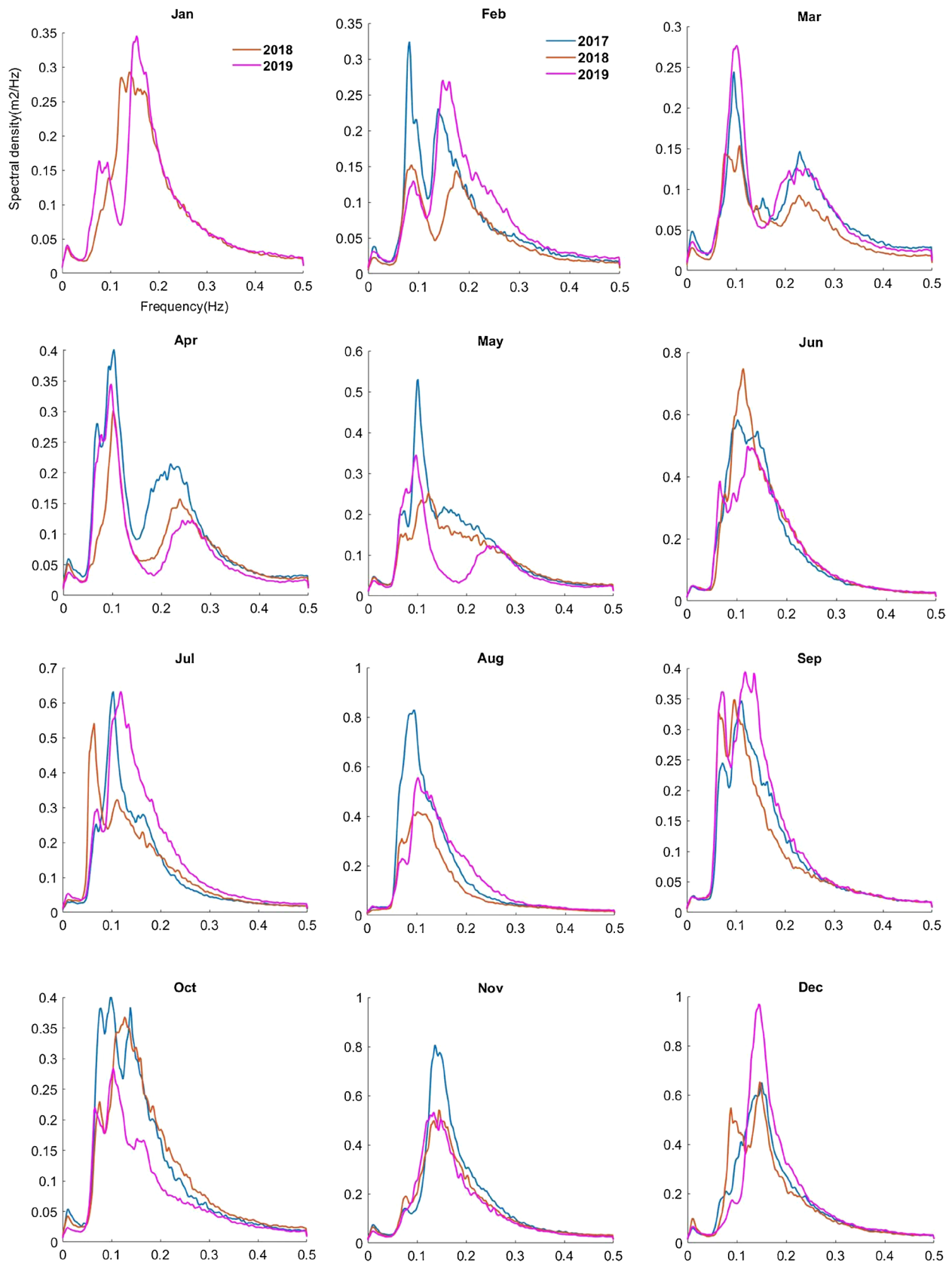


Fig. 7 Monthly averaged wave spectrum of frequency (Hz) versus spectral density (m^2/Hz) for years 2017, 2018, and 2019

Table 1 Monthly averaged spectrum separation/swell/wind sea frequency and related energy during the pre-monsoon (FMAM)

S.No			2017		2018		2019	
			Frequency (Hz)	Energy (m ² /Hz)	Frequency (Hz)	Energy (m ² /Hz)	Frequency (Hz)	Energy (m ² /Hz)
1	February	Separation frequency	0.12	0.10	0.13	0.05	0.12	0.08
		Swell	0.08	0.32	0.09	0.15	0.09	0.13
		Wind sea	0.14	0.23	0.18	0.14	0.15	0.27
2	March	Separation frequency	0.17	0.06	0.19	0.05	0.15	0.05
		Swell	0.10	0.24	0.07,0.11	0.14,0.15	0.10	0.28
		Wind sea	0.23	0.15	0.23	0.09	0.21,0.22	0.12,0.13
3	April	Separation frequency	0.15	0.09	0.16	0.06	0.18	0.03
		Swell	0.07,0.10	0.28,0.40	0.10	0.30	0.08,0.10	0.26,0.35
		Wind sea	0.22	0.21	0.24	0.16	0.26	0.12
4	May	Separation frequency	-	-	-	-	0.18	0.03
		Swell	0.07, 0.10	0.20, 0.53	0.08,0.12	0.14,0.25	0.10	0.35
		Wind sea	-	-	-	-	0.26	0.12

Sanil Kumar 2020), inter-annual and inter-seasonal variability of wind seas and swells in the Indian Ocean (Sreelakshmi and Bhaskaran 2020a). ERA5 also provides 2-dimensional wave spectra with 24 directions and 30 frequencies.

Methods

FFT is a discrete Fourier transform, which changes discrete signal to frequency domain from its time domain. Wave record data collected for 1024 s are applied on FFT

using MATLAB. It is divided into 256 segments with 50% overlapping the periodograms are computed using Hamming window. The periodogram frequency ranges from 0 to 0.5 Hz with an even number of discrete Fourier transform points. The spectrum was obtained by combining the FFT of 8 series, each of which contained 256 observations of vertical heave data.

Wave parameters such as significant wave height (Hm0) and mean wave period (Tm02) were obtained from the spectral moment. Significant wave height (Hm0), can be

Table 2 Monthly averaged spectrum separation/swell/wind sea frequency and related energy during the monsoon (JJAS)

S.No			2017		2018		2019	
			Frequency (Hz)	Energy (m ² /Hz)	Frequency (Hz)	Energy (m ² /Hz)	Frequency (Hz)	Energy (m ² /Hz)
1	June	Separation frequency	-	-	-	-	-	-
		Swell	0.10	0.58	0.11	0.75	0.06,0.12	0.39, 0.50
		Wind sea	0.14	0.55	-	-	-	-
2	July	Separation frequency	-	-	-	-	-	-
		Swell	0.10	0.63	0.06, 0.11	0.54, 0.32	0.07,0.12	0.30, 0.63
		Wind sea	-	-	-	-	-	-
3	August	Separation frequency	-	-	-	-	-	-
		Swell	0.10	0.83	0.10	0.42	0.10	0.55
		Wind sea	-	-	-	-	-	-
4	September	Separation frequency	-	-	-	-	-	-
		Swell	0.07,0.11	0.25,0.35	0.06,0.10	0.32, 0.35	0.07,0.12	0.36,0.39
		Wind sea	-	-	-	-	0.13	0.39

Table 3 Monthly averaged spectrum separation/swell/wind sea frequency and related energy during the post-monsoon (ONDJ)

S.No			2017		2018		2019	
			Frequency (Hz)	Energy (m ² /Hz)	Frequency (Hz)	Energy (m ² /Hz)	Frequency (Hz)	Energy (m ² /Hz)
1	October	Separation frequency	-	-	-	-	-	-
		Swell	0.08,0.10	0.38,0.40	0.07	0.23	0.07,0.10	0.22,0.28
		Wind sea	0.14	0.38	0.13	0.37	0.15	0.17
2	November	Separation frequency	-	-	-	-	-	-
		Swell	-	-	-	-	-	-
		Wind sea	0.14	0.81	0.14	0.54	0.13,0.15	0.53, 0.50
3	December	Separation frequency	-	-	-	-	-	-
		Swell	-	-	0.09	0.55	-	-
		Wind sea	0.15	0.65	0.15	0.65	0.14	0.97
4	January	Separation frequency	-	-	0.12	0.07	-	-
		Swell	0.12	0.28	0.08,0.09	0.16, 0.16	-	-
		Wind sea	0.14	0.29	0.15	0.35	-	-

estimated from the variance of a wave elevation record assuming that the wave spectrum is narrow. The variance can be calculated directly from the record or by integration of the spectrum as a function of frequency.

Significant wave height (H_m0) is given by $H_m0 = 4\sqrt{m_0}$

Mean wave period (T_{m02}), $T_{m02} = \text{Sqrt}\left(\frac{m_0}{m_2}\right)$

m_0 - Zeroth moment, m_2 - Second order moment.

The spectral moments are calculated from m_n is the n-th order spectral moment given by $m_n = \int_0^\infty f^n S(f) df$, $n=0,1,2,\dots$, $S(f)$ is the spectral energy density corresponding to frequency f .

The period corresponding to maximum spectral energy is referred to as be Peak wave period (T_p), obtained from the wave spectrum.

Mean wave direction (M_{dir}), $\theta_1 = \tan^{-1}\left(\frac{b_1}{a_1}\right)$, b_1 , a_1 are the Fourier coefficients (Earle 1996).

Wind seas and swells are identified and classified based on steepness parameter, GR ($GR = H_m0 / L$) into (i) sea ($0.083 < GR < 0.025$), (ii) young swell ($0.025 < GR < 0.01$), (iii) mature swell ($0.01 < GR < 0.004$), and (iv) old swell ($GR < 0.004$) based on Thompson et al. 1984 where L is the wavelength calculated for spectral peak period (T_p). Classification of wave spectrum based on seasons and inter-annual variability has been studied. The wave steepness algorithm adopted by the National Data Buoy Center (NDBC) is used for separation frequency from the monthly averaged spectrum (Gilhousen and Hervey

2001). This method determines a separation frequency by assuming that wind-seas are steeper than swell and that maximum steepness, occurs in the wave spectrum near the peak of wind-seas energy. The wind data from the moored buoy (CB06) is used for the year 2019 to study the land and sea breeze effect. Observations during the passage of two cyclones Gaja and Phethai have been analyzed in detail (Fig. 1). To verify the results of moored buoy CB06, wave parameters like significant wave height and mean wave period are validated with measurements made from a nearby DWR buoy called PP WET buoy. Wave parameters like significant wave height and mean wave period of reanalysis data of ERA5 (Hersbach et al. 2020; Muhammed Naseef and Sanil Kumar 2020) have been compared with the observations of CB06 moored buoy parameters.

Reanalysis results are statistically compared with moored buoy data (CB06) using Pearson's linear correlation coefficient (R), BIAS, Root Mean Square Error (RMSE), and scatter index (SI) (Amrutha et al. 2016).

Pearson's linear correlation coefficient (R) To quantify the relation between reanalysis and measured values, the correlation coefficient measures the strength and direction of the relationship between two variables. The directionality of the estimate is represented by the resultant sign. When both reanalysis and measured values change in the same direction, there is a positive or direct correlation; when one set of the reanalysis or measured values increases while the other drops, there is a negative or inverse correlation.

Table 4 Comparison of the results of this study with previous studies

S.No	Location	Time	Data source	Energy* (m ² /Hz) Monsoon	Energy* (m ² /Hz) Nonmonsoon	Energy* (m ² /Hz) Annual	Maximum Energy (m ² /Hz)	Hmax (m)	Annual* Hm0 (m)	Reference
1	off Ratnagri	2010-2014	DWR	3.28	0.24	1.25		4.2	1.2	Anjali Nair and Kumar 2016
2	off Karwar	2015-2017	DWR	6.13	0.75	2.56		5.1	1.14	Aravind et al. 2021
3	off Vengurlia	2015-2017	DWR	5.45	0.50	2.12		5.1	0.98	Aravind et al. 2021
4	Eastern Arabian Sea-off Honnavar	2011	DWR	5.5	0.61	3.05		7.0	1.55	Kumar et al. 2014a
5	Eastern Arabian Sea-off Ratnagri	2011	DWR	6.4	0.49	3.44		7.0	1.13	Kumar et al. 2014a
6	off Gangavaram	2010	DWR	2.2	1.0	1.40		5.2	1.0	Kumar et al. 2014b
7	off Karwar west coast of India	2011-2015	DWR				8.0	5.0	1.06	Nair and Kumar 2017
8	Northwestern Bay of Bengal	2013-2015	DWR				>4.0	6.7	1.0	Anjali et al. 2018
9	Head Bay of Bengal	2016	SWAN model	0.61	0.25	0.74				Patra et al. 2019
10	Central west coast of India-Honnavar	2009-2012	DWR	4.8		~2.0		7.26		Sanil Kumar and Anjali Nair 2015
11	off Visakhapatnam	2011-2015	DWR	1.29			2.14			Umesh et al. 2019b
12	off Chennai	2017-2019	Moored buoy	0.54	0.40	0.45	0.97	4.0	0.92	The present study

*Average

$$R = \frac{\sum_{i=1}^N | (A_i - \bar{A}) (B_i - \bar{B}) |}{\sqrt{\sum_{i=1}^N | (A_i - \bar{A})^2 (B_i - \bar{B})^2 |}} \tag{1}$$

BIAS It is the measure of the average difference between reanalysis and measured values. The positive bias value shows reanalysis values are higher than the observed values. Negative bias values are negligible in comparison to higher values of R.

$$BIAS = \frac{1}{N} \sum_{i=1}^N (A_i - B_i) \tag{2}$$

RMSE It is a generalized form of standard deviation. The information regarding the spread of data and their inter-relationships can be used to calculate the overall residual variation. Hence, the RMSE is an absolute measure of the fit between reanalysis and measured data. Low RMSE values indicate a better fit of reanalysis data with measurements.

$$RMSE = \sqrt{\frac{1}{N} \sum_{i=1}^N (A_i - B_i)^2} \tag{3}$$

SI Expressed in percentage is another measure for expressing the closeness of results among reanalysis and measured values.

$$SI = \frac{RMSE}{\bar{B}} \tag{4}$$

Where A_i represents the parameter based on the reanalysis. B_i represents the measured parameter, N is the number of data points, and the overbar represents the mean value.

Results and discussions

Wave classification

To understand seasonal and annual wave climate, waves are classified into three categories based on the spectral peak period (Glejin et al. 2013) (Aboobacker et al. 2009) short period waves (Tp < 8 s), (Aboobacker et al. 2013) intermediate period waves (8 < Tp < 13 s), and (Amrutha et al. 2016) long period waves (Tp > 13 s).

Short period waves

Short period waves are produced 44% during the three years study period, with 40% during pre-monsoon and 65% during a post-monsoon season dominated by the young swell, mature swell, and wind sea (Fig. 3). High-frequency waves

Table 5 Range and average value of wave parameters during 2017, 2018, and 2019

Year	Period	Hm0 (m)	Average Hm0(m)	Tp (s)	Average Tp (s)	Mdir (deg)	Average Mdir (deg)
2017	Pre-monsoon	0.29–1.73	0.85	2.94–18.96	9.08	30–176	136
	Monsoon	0.52–1.78	1.02	3.91–18.96	10.07	86–177	143
	Post- monsoon	0.38–2.09	1.00	2.98–18.29	8.05	40–162	95
2018	Pre-monsoon	0.35–1.89	0.72	2.80–21.33	8.60	59–165	119
	Monsoon	0.50–2.11	0.95	3.51–18.96	10.56	28–190	135
	Post- monsoon	0.40–2.90	0.95	2.75–16.52	7.88	24–175	99
2019	Pre-monsoon	0.36–2.07	0.84	2.78–18.29	8.55	68–183	127
	Monsoon	0.53–1.97	1.04	3.37–18.96	9.53	25–178	142
	Post- monsoon	0.40–1.97	0.98	3.16–18.29	8.18	35–175	102

are highest during post-monsoon due influence of NW monsoon. The direction of these waves during pre-monsoon is SE direction, and post-monsoon is predominant in the East-erly direction (Fig. 4). The percentage of short period waves

is less during monsoon (27%) as a result, the domination of young and mature swells approach in the direction of SE. During the three seasons, the mean wave period differed between 3.54 and 7.56 s, and the primary wave height ranged from 0.39 to 2.31 m.

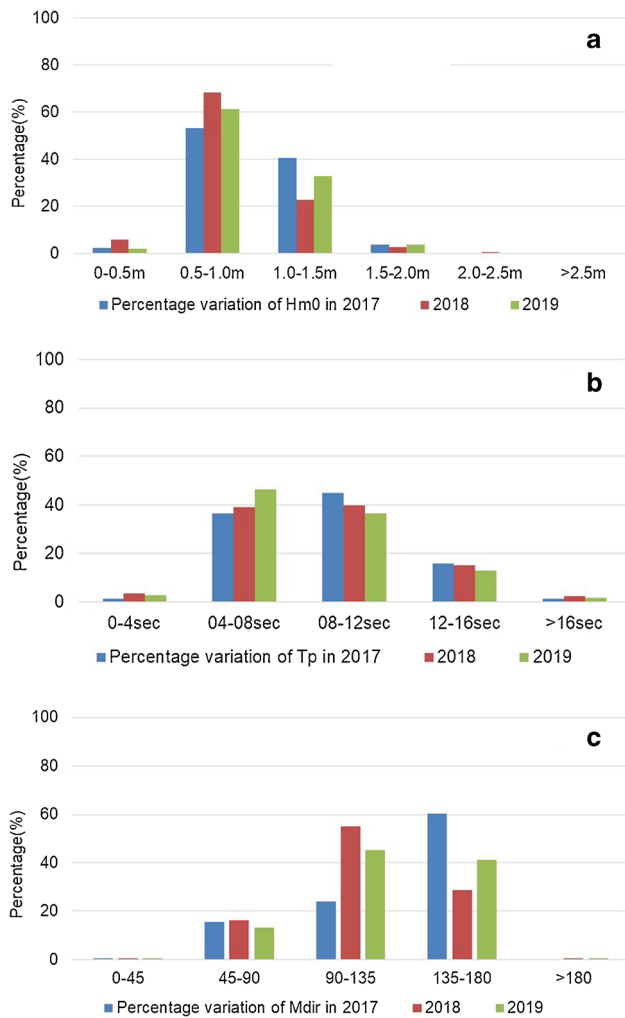


Fig. 8 Percentage variation of **a** significant wave height (Hm0), **b** peak wave period (Tp), and **c** mean wave direction (Mdir) shown for 2017, 2018, and 2019

Intermediate period waves

Intermediate period waves are produced 43% during the three years study period. These waves were frequently formed during the monsoon, which is characterized by young, mature, and old swells followed by, pre-monsoon and monsoon (Fig. 3). The pre-monsoon and monsoon direction of these waves is SE (Fig. 5), and their major wave height ranges from 0.29 to 2.90 m with a mean wave period of 3.90–9.72 s.

Long period waves

Long period waves are generated for 13% during the study period. Glejin et al. 2013 studied wave climate over the near shore waters off Puducherry, southwestern Bay of Bengal, and found long period waves were observed for 5% during 2009–2011. Shows the influence of Southern Ocean swells is higher in the present location. Long period waves are less than 7% during January, May, November, and December: Maximum in September (30%), followed by October, July, April, August, February, March, and June (Fig. 3). These swells originated from the Southern Ocean and modified the changes near the coast (Nayak et al. 2013). A higher percentage (18%) of long period waves are observed in SW monsoons dominated by old swells, and the direction of these waves is southeast. This Southern Ocean swells also show a common approach of propagation SE during monsoon and pre-monsoon (Fig. 6). The mean wave period changes from 4.03 to 10.26 s, and the significant wave height from 0.39 to 1.77 m. These waves are observed to have a considerable wave height of less than 2.0 m. (Kumar et al. 2014b).

Table 6 Seasonal average value of wave parameters during the entire study period

Year	Period	Average Hm0 (m)	Average Tp (s)	Average Mdir (deg)
2017, 2018 & 2019	Pre-monsoon	0.80	8.74	127
	Monsoon	1.0	10.05	140
	Post-monsoon	0.82	8.03	99

Inter-annual variations in monthly averaged wave spectra of CB06

The monthly averaged wave spectrum (Fig. 7) for coastal Chennai for a period of 3 years (from 2017 to 2019) is analyzed to study the temporal, seasonal, and inter-annual variations of spectral energy density.

During pre-monsoon (FMAM), the monthly averaged spectrum (Fig. 7) shows that the swells are dominating with peak energy corresponding to frequency values varying from 0.07 Hz ($T_p=14.28$ s) to 0.12 Hz ($T_p=8.33$ s). In February 2019, the peak energy in the wind sea frequency of 0.15 Hz (Table 1) was because of the sea breeze (Umesh et al. 2019a). The wave spectrum is said to have a double peak during the pre-monsoon, where the primary peak value is in the swell and the minor peak value is in the wind sea from February to May (Table 1). The Southern Indian Ocean waves and local winds contribute to the double peak wave spectrum (Sandhya et al. 2014).

During SW monsoon (JJAS), the wave spectrum shows a double/single peaked spectrum. The spectral peak energy ranges between 0.06 and 0.12 Hz (Table 2) during the monsoon season. It is comparable to the northern BoB peak (Kumar et al. 2014b), which is around 0.065–0.12 Hz, but different from the northeast Arabian Sea peak (Anjali Nair and Kumar 2016), which was around 0.08–0.12 Hz. The secondary peak changes from 0.06 to 0.08 Hz (16.67–12.5 s) (Tables 1, 2 and 3) are noticed in the swell for January, March–July, and September–October because of long period waves from the Southern Indian Ocean (Sandhya et al. 2014). The swell dominated double peaked spectra

secondary peak frequency ranged from 1.1 to 2.0 times the primary peak frequency, with an average value of 1.5 and less than the value (2.2) observed by Kumar et al. 2014b. During March–May, the wind sea peak is in the high frequency range of >0.2 Hz, but it is lower at other times of the year. In the post-monsoon (ONDJ), averaged spectrum shows a single peak with wind sea domination caused by the onset of NE monsoon and low-pressure system in BOB (cyclone, depression). Peak energy corresponding to the frequency between 0.13 and 0.15 Hz shows wind sea domination. During October, swells are dominating compared with the wind sea because of weak local winds. In November, secondary peak is observed in the wind sea at 0.15 Hz (Table 3). The study findings show a wide range of spectral types along the southwest BoB, including (1) single peaked spectra, (2) swell dominated double peak spectra, and (3) wind sea dominated double peak spectra. Interannual variations were observed for the monthly averaged wave spectrum in all months except August. In August, peak frequency is 0.10 Hz for all the years. The monthly averaged wave spectrum shows a double peak spectrum during the pre-monsoon and transition period during NE and SW monsoon. The occurrence of double peaked spectrum, for 60% in the shallow water of the Indian coast (Kumar et al. 2003) and during low energy state conditions (Umesh et al. 2019a). The combination of wind sea and swells (young swells and mature swells) produce double (or multi-peaked) spectra (Aboobacker et al. 2009). Most of the peak energy is concentrated in the low frequency region (<0.12 Hz) indicate, that swells are dominate in all seasons except during November–December. During pre-monsoon, monsoon, and post-monsoon seasons, peak energy differs from 0.15 to 0.53 m^2/Hz , 0.35 to 0.83 m^2/Hz , and 0.28 to 0.97 m^2/Hz . The energy value is less than 1 m^2/Hz during the study period indicating a low energy state compared with the northwestern Bay of Bengal (Gopalpur) where the monthly averaged wave spectrum shows up to 4 m^2/Hz (Anjali et al. 2018). The annual spectral energy (average of monthly maximum) density varies from 0.40 (2018) to 0.52 m^2/Hz (2017). The current location has a lower energy state than the other studies, as demonstrated in Table 4.

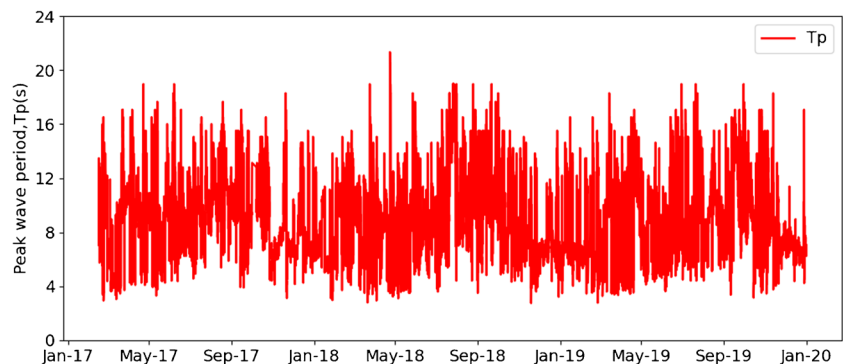
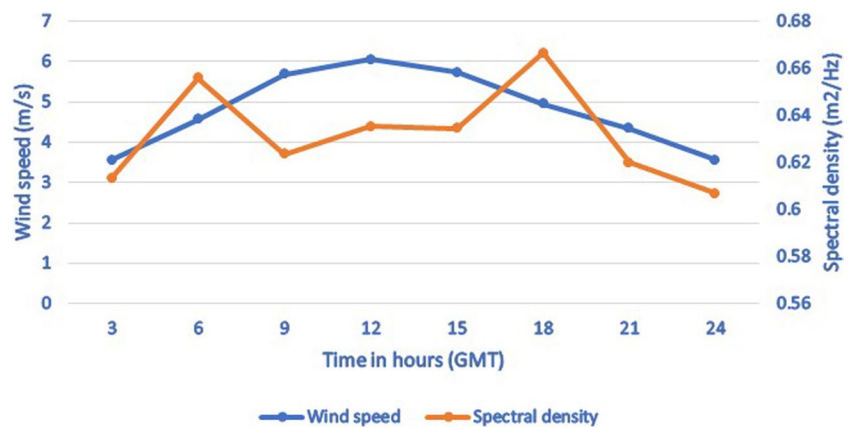
Fig. 9 Peak wave period for the year 2017–2019

Fig. 10 Hourly variation of monthly averaged wind speed and spectral density for February



The peak energy corresponding frequency of swell/wind sea and separation frequency is shown in the Tables 1, 2 and 3. The separation frequency is based on wave steepness algorithm followed by the National Data Buoy Center (NDBC) which separates wind sea and swell from the wave spectrum (Gilhousen and Hervey 2001).

Wave spectral parameters

Table 5 shows the average value of wave parameters. In three years, period H_m0 remains almost the same during all seasons. During monsoon and post-monsoon, the average value of H_m0 is ~ 1.0 m. South of the present study, Puducherry and Cuddalore show that mean significant height is higher in NE monsoon, and lower in SW monsoon and pre-monsoon (Glejin et al. 2013; Jena et al. 2017). The percentage distribution of significant wave height shows 0–0.5 m equals 3%, 0.5–1.0 m equals 61%, 1.0–1.5 m equals 32%, and the rest of the waves are more than 1.5 m (Fig. 8a). According, to a study performed on the southeast coast of Tamilnadu during one year for H_m0 shows 0–0.5 m represents 17%, 0.5–1.0 m represents 60%, and > 1.0 m represents 23% (Jena et al. 2017). The present study shows the H_m0 is greater than 1.0 m for 36% and < 0.5 m for 3% it is due to the influence of

swells that the significant wave height is increased (Nayak et al. 2013). The mean significant wave height in Kalpakkam is 0.7 m as a result of the wind sea effect. The H_m0 increases to 1.3 m by considering swells. It shows the remote ocean swells effect the wave activity in the southwest Bay of Bengal (Nayak et al. 2013).

The average peak wave period in pre-monsoon is 8.74 s, monsoon is 10.05 s, and post-monsoon is 8.03 s (Table 6); these indicate swells are dominating in all seasons but whereas, in Cuddalore coastal location shows swells are noticed during SW monsoon ($T_p = 10.1$ s) and wind seas ($T_p = 7.1$ s) in pre-monsoon (Jena et al. 2017). This shows the influence of Southern Ocean swells is higher in coastal Chennai in comparison to Puducherry and Cuddalore. The peak period (T_p) in the range of 0–8 s (43%) and 8–21.33 s (57%) (Fig. 8b) shows wind sea dominated and swell dominated spectra. Southern Ocean swells are observed in the Arabian Sea and Bay of Bengal when the peak period is 12 s (Nayak et al. 2013). This typical wave period is observed in all seasons (Table 5) of the study during all months (Fig. 9). The Southern Ocean swells move eastward, then when they reach western Australia, they broaden out and move northwest till they reach the northern Indian Ocean (Nayak et al. 2013). During the study period, 84% of the waves approach

Fig. 11 Hourly variation of monthly averaged wind direction for February

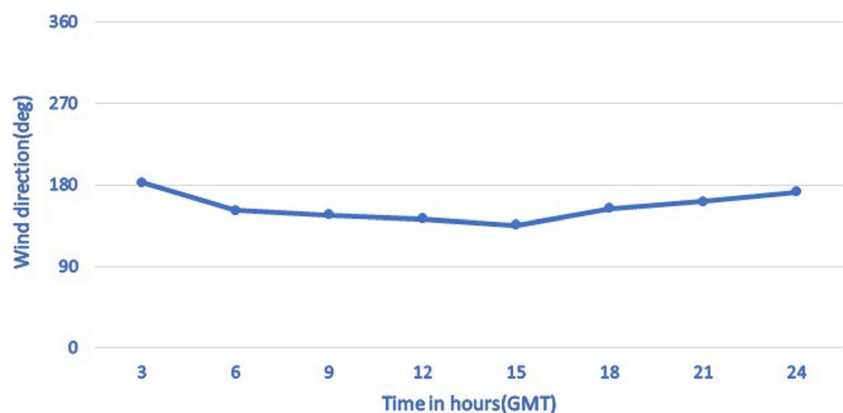
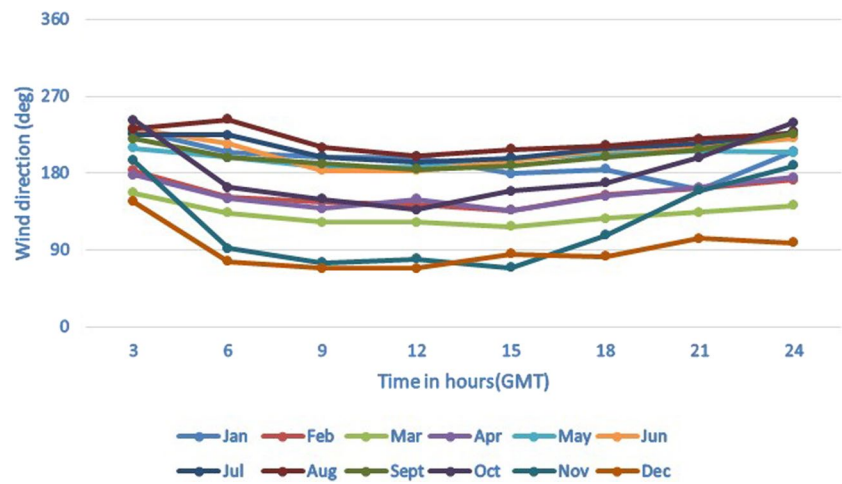


Fig. 12 Hourly variation of monthly averaged wind direction for the year 2019



from SE/ESE, and the remaining are from the ENE direction (Fig. 8c). Seasonal average of mean wave direction is from 100 to 140° (Table 6).

The annual average significant wave height in 2017 was 0.96 m. In 2018 is 0.87 m, and in 2019 is 0.94 m. Karwar, the yearly significant wave height is 1.14 m (Aravind et al. 2021), 0.81 m (Jena et al. 2017) for the southeast coast of India, and 1.0 m for northern BoB (Kumar et al. 2014b), and northwestern BoB (Anjali et al. 2018). Kumar et al. 2004 studied wave characteristics off the Visakhapatnam coast and observed that significant wave height is 1.0–3.0 m during May– September, 0.5–2.0 m during October–December (except during cyclones), and wave period varies from 9 to 12 s for a major period of the year. The average significant wave height during monsoon is 1.45 m, and post-monsoon is 1.06 m in the northern BoB (Kumar et al. 2014b). According to Patra et al. 2016, the average significant wave height in the northwestern BoB is 1.49 m during the monsoon and 0.88 m in the NW monsoon. These indicate that Hm0 increases toward the north of the BoB, while it decreases in the southwest of the BoB because of the reduced effect of the SW monsoon. However, in Chennai, Hm0 is higher than in Puducherry and Cuddalore due to the significant

influence of Southern Ocean swells in the study area. The current location has a lower significant height than other studies, as shown in Table 4.

Sea and land breeze circulation

Sea breeze circulations occur along coastal regions due to the contrast between surface temperatures over land and water. The sea/land breeze system affects the wave spectrum's physical process. The wind and wave measurements for 2019 have been used and analyzed during pre-monsoon, monsoon, and post-monsoon. The wind speed in February is 3.54 m/s around 03:00 h GMT, a maximum of 6.04 m/s during 12:00 h GMT and then slowly decreases to 3.54 m/s around 24:00 h GMT (Fig. 10). In February, the wind direction changes from south to southeast as a sea breeze develops at 09:00 GMT at 145° and lasts until 15:00 GMT (Fig. 11). Around 24:00 GMT, the direction returns to southerly caused by the weakening of the sea breeze (Fig. 11). The observed time difference between maximum wind speed and wave spectral energy is 5–6 h (Fig. 10). During monsoon and post-monsoon, the effect of sea-land breeze is minimum (Figs. 12 and 13). The

Fig. 13 Hourly variation of monthly averaged significant wave height (m)

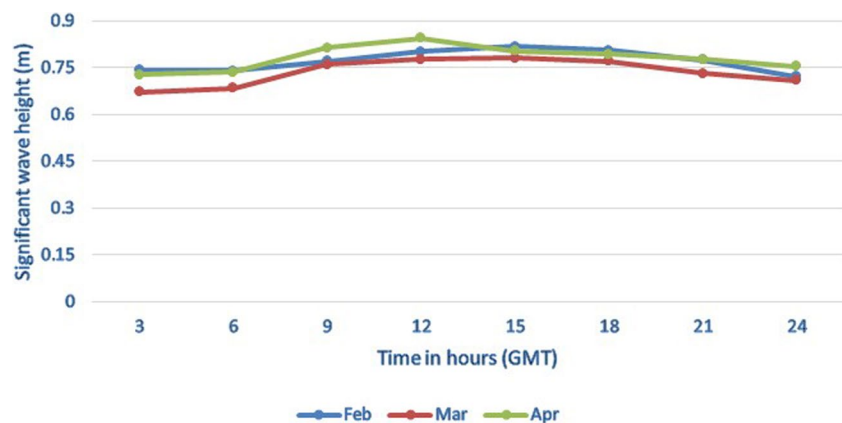
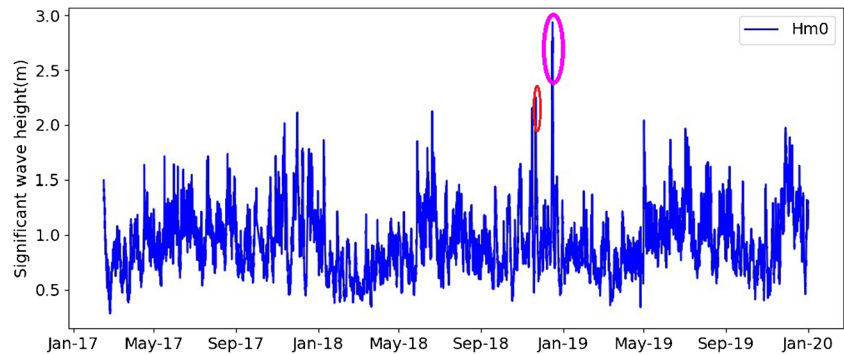


Fig. 14 Wave spectra observed during (a–c) very severe cyclonic storm- Gaja and (d–f) severe cyclonic storm- Phethai



effect of the sea breeze is observed from February–April, higher during March, and shows an increase in significant wave height during 12:00 h (GMT) (Fig. 13).

Variation of sea state during cyclone and depression

Tropical cyclone causes significant changes in ocean wave characteristics and propagation (Chu and Cheng 2008). This spectral energy is used for the design and safe operations of ships, and significant wave height during a cyclone is used in the design of harbors. During a cyclone, the significant wave height is used to validate numerical models of shallow water depth.

We observed higher wave energy of 0.8 m²/Hz to a frequency of 0.14 Hz in November 2017 due to the depression

formation over west-central BoB off the Andhra Pradesh coast (15–17 November 2017).

Very severe cyclonic storm- Gaja (10–19 November 2018) intensified into a Severe Cyclonic Storm (SCS) over southwest BoB in the morning (0830 IST) of 15 November and into a very severe cyclonic storm on the same night (2030 IST). The cyclone crossed Tamil Nadu and Puducherry coasts between Nagapattinam and Vedaranniyam (10.45° N, 79.80° E) from 1900 to 2100 GMT on 15 November 2018. The cyclone's peak maximum sustained surface wind speed (MSW) was 130 kmph gusting to 145 kmph from 1800 to 2100 GMT on 15 November 2018. The lowest estimated central pressure was 975 hPa, with a pressure drop of about 31 hPa (IMD 2018a).

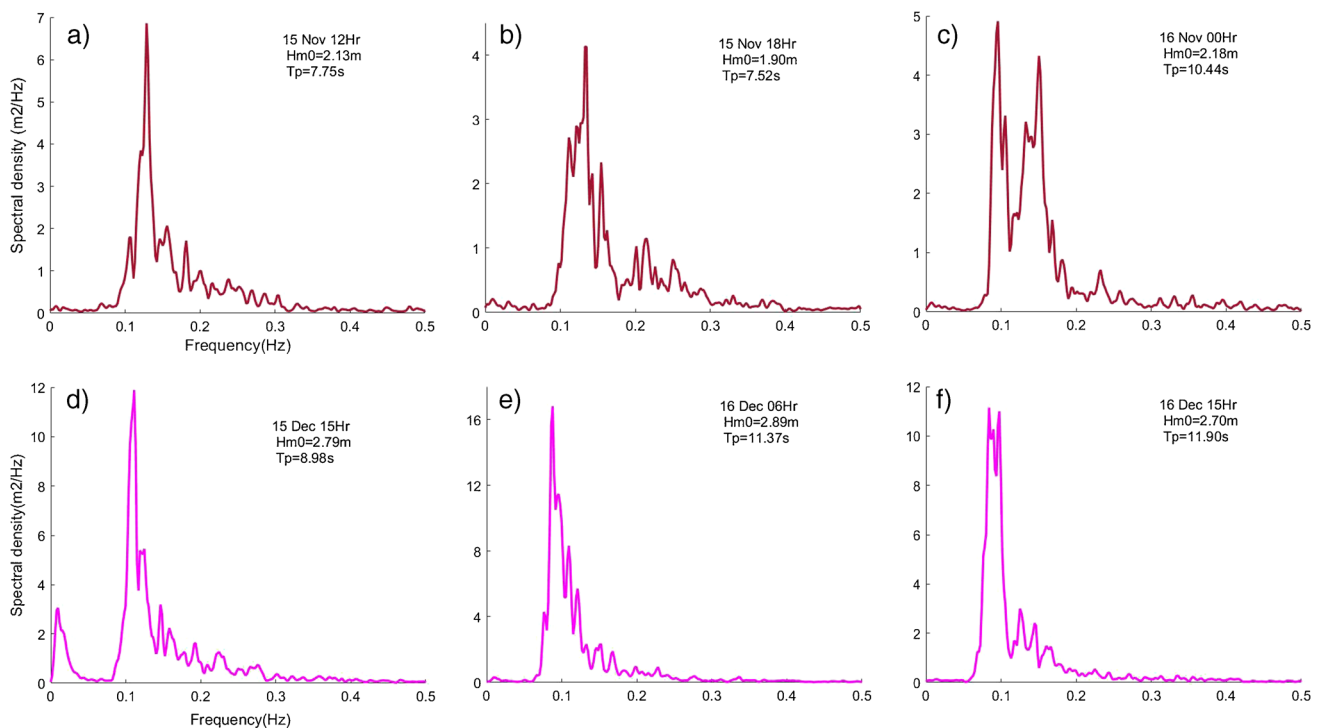


Fig. 15 Daily averaged spectra during cyclone period Gaja

Fig. 16 Significant wave height observed during cyclonic storm of Gaja and Phethai

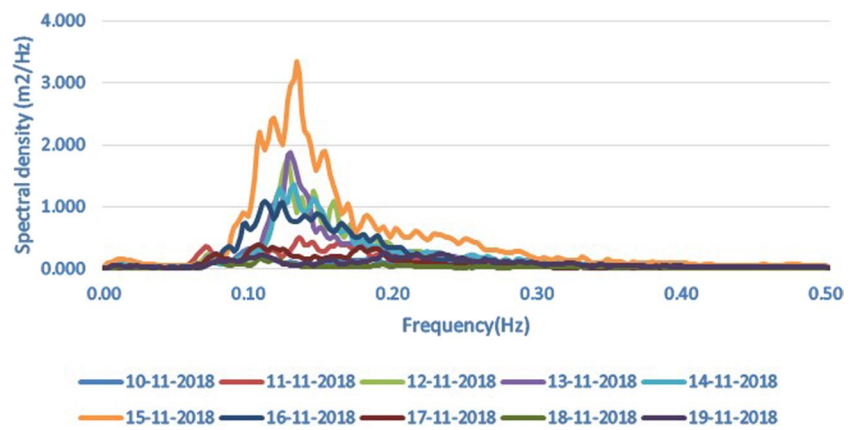
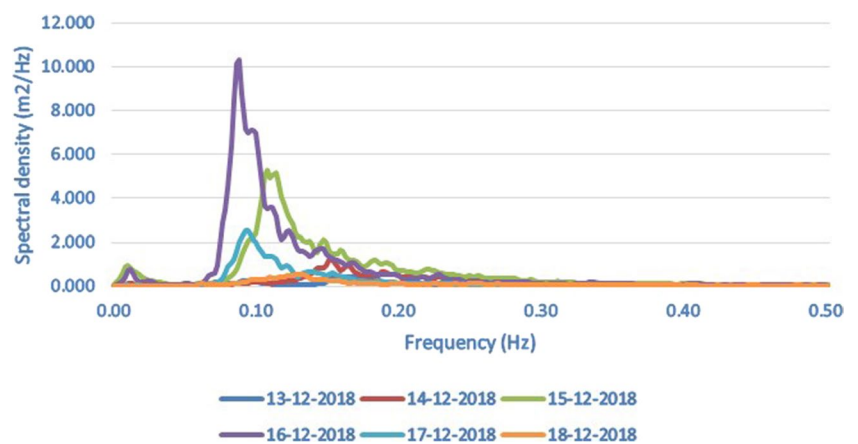


Fig. 17 Daily averaged spectra during cyclone period Phethai



During the Gaja cyclone period, spectral energy density varied from 0.08 to 7.0 m²/Hz, the peak period changed between 3 and 15 s, and significant wave height ranges from 0.5 to 2.2 m. The maximum energy observed during the cyclone is 7.0 m²/Hz (Fig. 14a–c) with single peak wind sea domination. During the crossing, the buoy location from the respective cyclone track is ~290 km. The peak period varies from 7 to 10 s during 14–15 November 2018 (Fig. 15). These show intermediate period waves were observed, in the north Indian Ocean cyclones (Glejin et al. 2013). Thompson et al. 1984, the steepness parameter Hm₀/L during the cyclone period reveals 95% swells and 5% wind sea. Young swells dominated the wave field during 11–16 November

2018. These were caused by swells that were produced by the cyclone's strong wind field and propagated in a forward direction as it moved. It is a regular phenomenon during tropical cyclones (Young 2006). The daily averaged wave spectra are shown in Fig. 15. The spectrum shows energy spreading from 0.10 to 0.20 Hz during 12–14 November 2018. During the cyclone crossing on 15 November 2018, broader frequency range was 0.08–0.30 Hz because the peak shifted toward the high frequency of wind sea during the landfall of a cyclone (Fig. 15). The observed Hm₀ during the passage of Gaja cyclone 2.2 m (Fig. 16) and Hmax is 3.17 m. The Hm₀ observed during the passage of the Jal cyclone is 2.5m on the Puducherry coast (Glejin et al. 2013). The wave spectrum is flat after cyclone crossing, and energy is reduced, broader frequency range, the significant wave height is reduced to 0.96 m after 24 h of cyclone passage.

Table 7 Statistics for significant wave height (Hm₀) and mean wave period (Tm₀₂) of PP WET buoy in comparison to CB06 buoy parameters

Year	Parameter	R	RMSE	SI	BIAS
2017	Significant wave height (m)	0.96	0.065	0.07	-0.002
2018	Significant wave height (m)	0.96	0.09	0.095	0.004
2019	Significant wave height (m)	0.95	0.068	0.08	0.019
2018	Mean wave period (s)	0.91	0.49	0.083	0.063
2019	Mean wave period (s)	0.86	0.46	0.089	0.16

Severe cyclonic storm- Phethai (13–18 December 2018) enhanced into a deep depression (DD) over south-east BoB at midnight (2330 IST) of 13 December 2018. It intensified into a cyclonic storm (CS) Phethai in the evening (1730 IST) of 15 December and into a severe cyclonic storm (SCS) in the afternoon of 16 December. It maintained its intensity of SCS till the early morning of

Fig. 18 Comparison of moored buoy (CB06) and PP WET buoy for significant wave height in 2017

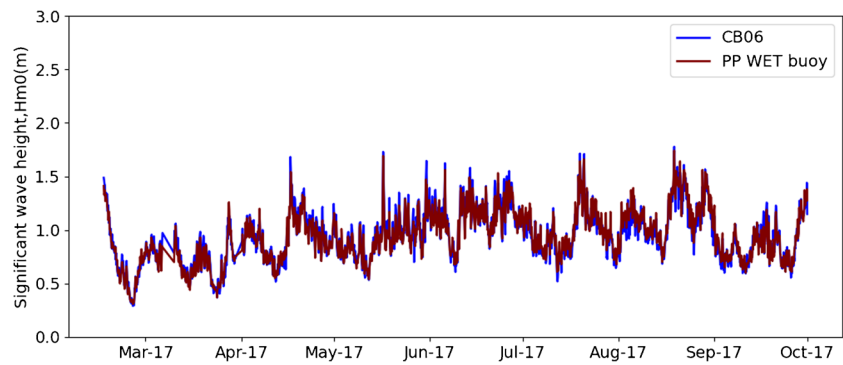
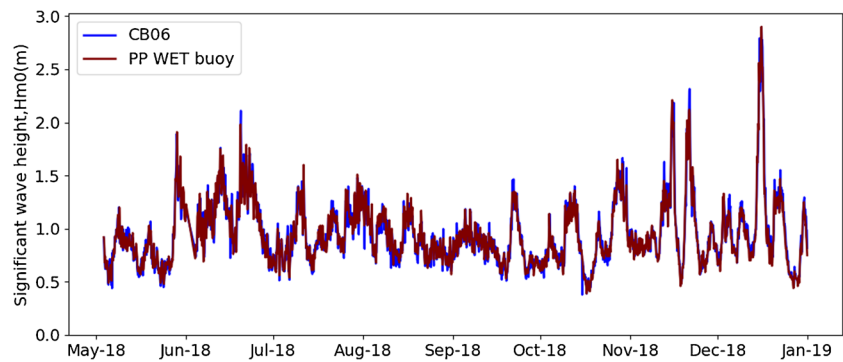


Fig. 19 Comparison of moored buoy (CB06) and PP WET buoy for significant wave height in 2018



17 December and weakened into a cyclonic storm in the morning. Moving north-northwestwards and then northwards, it crossed the Andhra Pradesh coast near 16.55° N and 82.25° E from 08:00 to 09:00 hrs GMT on 17 December 2018. The cyclone's peak maximum sustained surface wind speed (MSW) was 100–110 kmph gusting to 120 kmph (55 knots) from 1200 to 2100 GMT on 16 December 2018. The lowest estimated central pressure was 992 hPa during the same period, with a pressure drop of 15 hPa (IMD 2018b).

During the Phethai cyclone, the spectral energy density and significant wave height increased from 0.4 to $17.0 \text{ m}^2/\text{Hz}$ and 0.74–2.90 m. The cyclone close to the measurement location (257–400 km) on 16 December 2018 (06:00–21:00 h GMT), T_p ranges from 11 to 12 s, and H_{m0} varies between

2.25 and 2.90 m. The maximum energy observed during the cyclone is $17.0 \text{ m}^2/\text{Hz}$ (Fig. 14d–f) with single peak swell domination. The observed H_{m0} and H_{max} were 2.90 m (Fig. 16) and 4.0 m before cyclone landfall on 16 December 2018 at 06:00 h GMT. Before the landfall of cyclone Jal, the observed H_{m0} and H_{max} off the Cuddalore coast were 2.14 m and 5.7 m (Jena et al. 2017). Thompson et al. 1984, the steepness parameter H_{m0}/L during the cyclone period reveals 96% swells and 4% wind sea. The daily averaged wave spectra are shown in Fig. 17. The wave spectrum (15–17 December 2018) shows swell domination with varying frequencies of 0.088–0.107 Hz and energy spreading between 0.06 and 0.20 Hz. Hence, the wave field is dominated by swells during the cyclone period. During cyclonic storms swell energy is higher than the wind seas (Kumar

Fig. 20 Comparison of moored buoy (CB06) and PP WET buoy for significant wave height in 2019

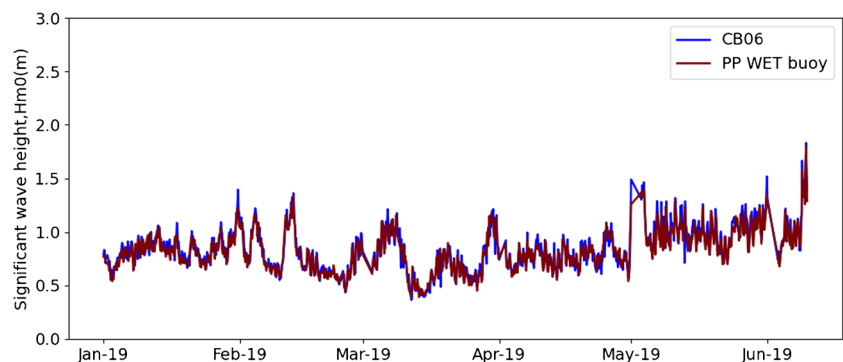
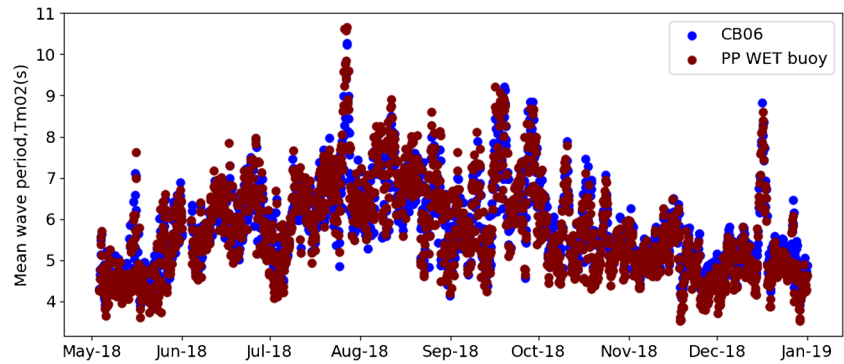


Fig. 21 Comparison of moored buoy (CB06) and PP WET buoy for mean wave period in 2018



et al. 2014b). After the cyclone crossing wave spectra flat, energy is reduced, and H_m0 after 24 h of passage is 0.89 m.

Comparison of moored buoy data with PP WET buoy and ERA5

The comparison statistics for 2017–2019 are shown in Table 7. PP WET buoy results and moored buoy shows a strong positive correlation coefficient of the order 0.95–0.96 for H_m0 and 0.86–0.91 for T_m02 . The negative bias of -0.002 and positive bias of 0.004 , 0.019 , and 0.063 are negligible, in addition to the higher value of R . The positive bias of 0.16 indicates a slight overestimation of moored buoy results (Umesh et al. 2018) the range of T_m02 (2019) for measured buoy ranges from 3.81 to 9.31 s, and PP WET buoy ranges from 3.44 to 8.96 s; there is 4–10% overestimation of results. The low values of SI for H_m0 and T_m02 indicate a better fit between the moored buoy and the PP WET buoy. RMSE for H_m0 varies from 0.065 to 0.09 m (6.5–9 cm). The manufacturer (Kongsberg) of Seatex MRU-6 has given dynamic accuracy of 5 cm, and the values show very minimal deviation from the standard PP WET buoy. RMSE for the mean wave period is less than 0.5 s. H_m0 and T_m02 showed a minimal variation from the actual values, which discloses a better agreement between PP WET and moored buoy. Figures 18, 19, 20, 21 and 22 show the comparison plots

of the PP WET buoy and the moored buoy (CB06) for the parameters significant wave height (m) and mean wave period (s).

Significant wave height (H_m0) and maximum wave height (H_{max}) of ERA5 are validated with moored buoy observations in AS and BoB (2 coastal and 2 deep water buoys). It shows a good agreement with moored buoy data in the coastal (bias ~ 0.29 m) and deep waters (bias ~ 0.18 m). ERA5 data is underestimated during cyclones, with a significant bias value of 0.69 m. (Muhammed Naseef and Sanil Kumar 2020). The coastal buoys of the central west coast of India are validated with ERA5 data for various wave parameters of significant wave height and maximum wave height. The correlation coefficient for H_m0 is 0.98 and 0.97 for H_{max} . The bias varies from 0.08 to 0.18 m for H_m0 and 0.55 to 0.67 m for H_{max} (Aravind et al. 2021). ERA5 data shows a high correlation coefficient for comparison with coastal and deep-water buoys in the Indian Ocean (Muhammed Naseef and Sanil Kumar 2020; Aravind et al. 2021).

The comparison statistics for 2017–2019 are shown in Table 8. Moored buoy results and ERA5 reveal a positive correlation coefficient of the order 0.85–0.90 for H_m0 and 0.57–0.71 for T_m02 . Lower values of SI and RMSE for H_m0 , indicating a good fit between ERA5 and moored buoy. The positive bias of H_m0 signifies that ERA5 results are slightly higher than a moored buoy. The

Fig. 22 Comparison of moored buoy (CB06) and PP WET buoy for mean wave period in 2019

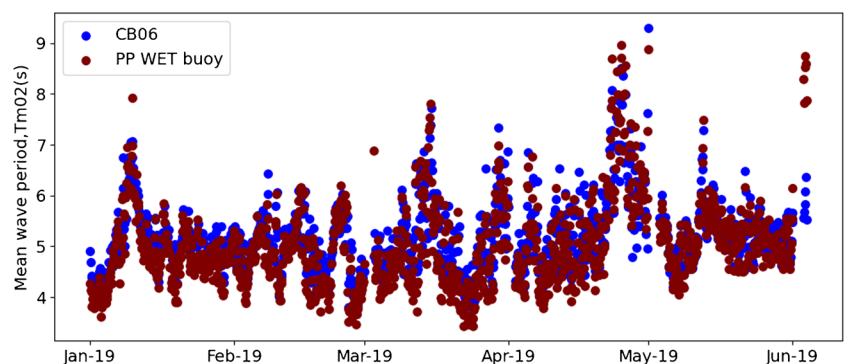
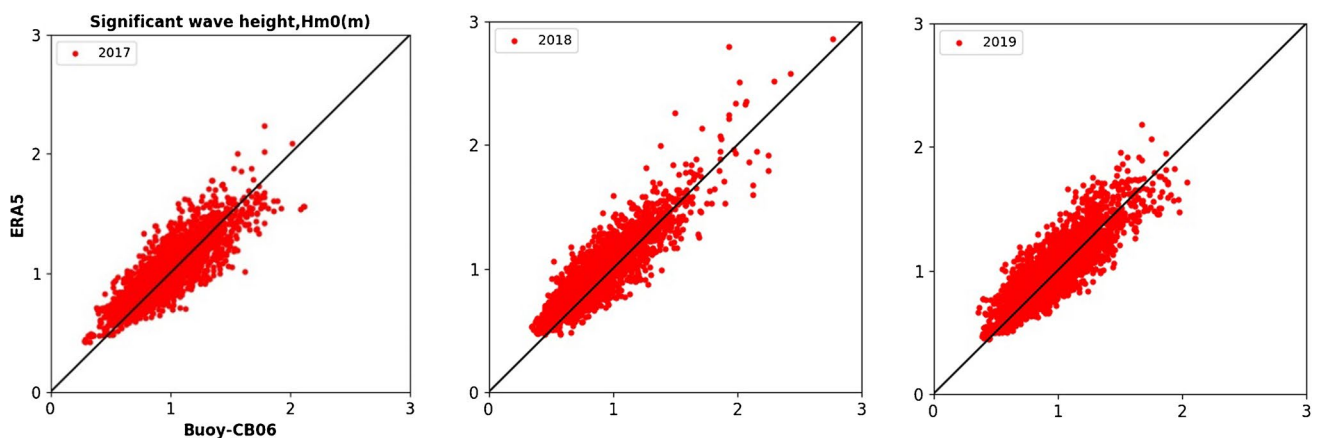
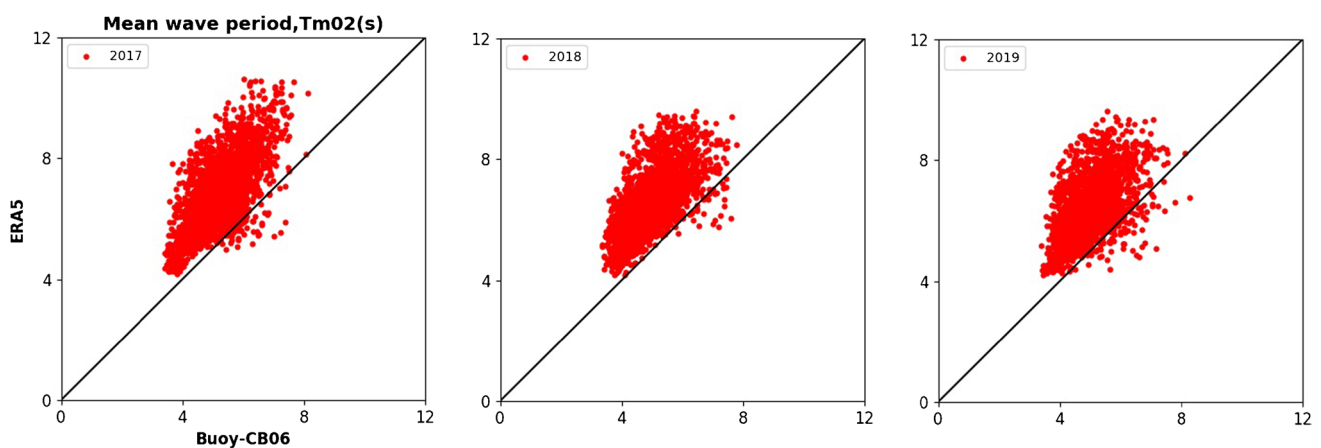


Table 8 Statistics for significant wave height (m) and mean wave period (Tm02) of reanalysis data ERA5 in comparison to CB06 buoy parameters

Year	Parameter	R	RMSE	SI	BIAS
2017	Significant wave height (m)	0.85	0.15	0.16	0.05
2018	Significant wave height (m)	0.90	0.16	0.18	0.084
2019	Significant wave height (m)	0.87	0.15	0.15	0.043
2017	Mean wave period (s)	0.71	1.8	0.35	1.57
2018	Mean wave period (s)	0.68	1.7	0.35	1.54
2019	Mean wave period (s)	0.57	1.6	0.33	1.38

significant wave height of ERA5 during cyclone Gaja is underestimated (-10%), and during Phethai, it is overestimated (+33%) with a higher bias of 0.843 m. The reanalysis shows satisfactory results over the entire year except during extreme events; it reveals a good comparison in shallow waters (16 m depth). Swain et al. 2017 studied a

similar study by validating the numerical model (WAM cycle 4.5.3) with moored buoy (off Chennai port) for Hm0 showed an R value of 0.93, SI is 0.05, BIAS value of -0.19, and RMSE value 0.04 during July 2000. It offers a good comparison because the reanalysis data of ERA5 uses the WAM model. Scatter plots of the moored buoy (CB06) and reanalysis (ERA5) plots for significant wave height are shown in Fig. 23. RMSE varied from 1.6 to 1.8 for Tm02, showing large deviations in reanalysis values. The positive higher bias for Tm02 indicates reanalysis values are overestimated during the entire period and fail to capture the seasonal variability of data. Higher values of SI for Tm02 show a 35% variation in the reanalysis data. The significant wave height reanalysis results exhibit seasonal variability, and Tm02 fails to capture it. However, peak values are overestimated significantly during extreme events. Scatter plots of the moored buoy (CB06) and ERA5 plots for the mean wave period are shown in Fig. 24.

**Fig. 23** Scatter plot of moored buoy and ERA5 data for significant wave height**Fig. 24** Scatter plot of moored buoy and ERA5 data for mean wave period

Conclusion

The wave spectral characteristics during 2017–2019 are studied based on measured wave data at 16 m water depth from moored buoy data off Chennai coast in the southwest Bay of Bengal. In 2017, 2018, and 2019, 13% of long period waves ($H_m0 < 2.0$ m) were observed, with a predominant SE wave direction considerably higher than in the coastal waters of Puducherry. Swell dominated double peaked spectra are observable in March through May, July, and September, while wind sea dominated double peaked spectra are seen in November. During the SW monsoon border, spectral peak ranges from 0.06 to 0.12 Hz due to the domination of swells from the south Indian Ocean and the Southern Ocean. The typical peak frequency is between 8 and 10 s, and the spectrum has a 57% swell dominance, demonstrating that swells are the predominant component in all seasons. Wave climate in monsoon differs from the coastal waters of Puducherry, Cuddalore, and the northeast Arabian Sea. From February–April, the afternoon H_m0 increases, which is a result of the sea breeze. Young and mature swells dominated the wave field during the cyclone. The maximum energy observed during the study is < 1 m²/Hz, indicating the low energy state compared with the northern Bay of Bengal. Verification of moored buoy data with PP WET buoy and reanalysis data of ERA5 shows a good correlation coefficient and low RMSE value. Reanalysis results of significant wave height exhibit seasonal variability. They are in good agreement during pre-monsoon, and the mean wave period shows overestimation during the substantial part of the study period. However, peak values during SW and NE monsoons are overestimated, especially during cyclone Phethai, which indicates the significance of measured spectra in validating models. Validating the measured spectrum against alternative theoretical wave spectra and the seasonal variations of the wind, sea, and swell waves is necessary for future research in the present location.

Acknowledgements The authors thank Director NIOT for his encouragement in carrying out this work. The authors express their sincere thanks to Ministry of Earth Sciences (MoES), Government of India for funding this project. The authors are very thankful to the Ocean Observation System (OOS) team for the buoy data from the moored buoy network.

Declarations

Conflict of interest The authors declare no competing interests.

References

- Aboobacker VM, Vethamony P, Sudheesh K, Rupali SP (2009) Spectral characteristics of the nearshore waves off Paradip, India during monsoon and extreme events. *Nat Hazards* 49(2):311–323
- Aboobacker VM, Vethamony P, Samiksha SV, Rashmi R, Jyoti K (2013) Wave transformation and attenuation along the west coast of India: Measurements and numerical simulations. *Coastal Engineering Journal* 55(1):1350001
- Amrutha MM, Kumar VS, Sandhya KG, Nair TB, Rathod JL (2016) Wave hindcast studies using SWAN nested in WAVEWATCH III-comparison with measured nearshore buoy data off Karwar, eastern Arabian Sea. *Ocean Eng* 119:114–124
- Amrutha MM, Sanil Kumar V, Anoop TR, Nair B, Nherakkol A, Jeyakumar C (2014) Waves off Gopalpur, northern Bay of Bengal during cyclone Phailin. In *Annales Geophysicae* 32(9):1073–1083
- Anjali Nair M, Kumar VS (2016) Spectral wave climatology off Ratnagiri, northeast Arabian Sea. *Nat Hazards* 82(3):1565–1588
- Anjali NM, Kumar VS, Amrutha MM (2018) Spectral wave characteristics in the nearshore waters of northwestern Bay of Bengal. *Pure Appl Geophys* 175:3111–3136
- Aparna M, Shetye SR, Shankar D, Shenoi SSC, Mehra P, Desai RGP (2005) Estimating the seaward extent of sea breeze from QuikSCAT scatterometry. *Geophys Res Lett* 32(13):L13601
- Aravind P, Amrutha MM, Kumar VS (2021) Ocean wave dynamics in the coastal area of the central west coast of India and its variability. *Ocean Eng* 227:108880
- Chu PC, Cheng KF (2008) South China Sea wave characteristics during Typhoon Muifa passage in winter 2004. *J Oceanogr* 64(1):1–21
- Dube SK, Rao AD, Sinha PC, Murty TS, Bahulayan N (1997) Storm surge in the Bay of Bengal and Arabian Sea: the problem and its prediction. *Mausam* 48(2):283–304
- Earle MD (1996) Nondirectional and Directional Wave Data Analysis Procedures. NDBC Technical Document 96-01(002):37
- Gilhousen DB, Hervey R (2001) Improved estimates of swell from moored buoys. In: *Proceedings of the Fourth International Symposium WAVES 2001*. ASCE, Alexandria, VA, pp 387–393
- Glejin J, Kumar VS, Nair TB (2013) Monsoon and cyclone induced wave climate over the near shore waters off Puduchery, south western Bay of Bengal. *Ocean Eng* 72:277–286
- Hanson JL, Phillips OM (2001) Automated analysis of ocean surface directional wave spectra. *J Atmos Oceanic Tech* 18(2):277–293
- Hersbach H, Bell B, Berrisford P, Hirahara S, Horányi A, Muñoz-Sabater J, Nicolas J, Peubey C et al (2020) The ERA5 global reanalysis. *Q J Roy Meteorol Soc* 146(730):1999–2049
- IMD (2018a) Very Severe Cyclonic Storm, “GAJA” over southeast Bay of Bengal (10 - 19 November 2018): a report. Cyclone Warning Division, India Meteorological Department, New Delhi
- IMD (2018b) Severe Cyclonic Storm, ‘PHETHAI’ over southeast Bay of Bengal (13 - 18 December 2018): a report. Cyclone Warning Division, India Meteorological Department, New Delhi
- Jena BK, Patra SK, Joseph KJ, Sivakholundu KM (2017) Seasonal variation in nearshore wave characteristics off Cuddalore, Southeast coast of Tamil Nadu, India. *Curr Sci* 112(10):2115–2121
- Johnson G, SanilKumar V, Sanjiv PC, Singh J, Pednekar PS, AshokKumar K, Dora GU, Gowthaman R (2012) Variations in swells along eastern Arabian Sea during the summer monsoon. *Open J Mar Sci* 2:43–50
- Kumar VS, Shanas PR, Dubhashi KK (2014a) Shallow water wave spectral characteristics along the eastern Arabian Sea. *Nat Hazards* 70(1):377–394
- Kumar VS, Dubhashi KK, Nair TB (2014b) Spectral wave characteristics off Gangavaram, Bay of Bengal. *J Oceanogr* 70(3):307–321
- Kumar VS, Kumar KA, Raju NSN (2004) Wave characteristics off Visakhapatnam coast during a cyclone. *Curr Sci* 86(11):1524–1529
- Kumar VS, Anand NM, Kumar KA, Mandal S (2003) Multi peakedness and groupiness of shallow water waves along Indian coast. *J Coast Res* 19(4):1052–1065
- Kumar VS, George J, Joseph D (2020) Hourly maximum individual wave height in the Indian shelf seas—its spatial and temporal variations in the recent 40 years. *Ocean Dynamics* 70(10):1283–1302

- Muhammed Naseef T, Sanil Kumar V (2020) Climatology and trends of the Indian Ocean surface waves based on 39-year long ERA5 reanalysis data. *Int J Climatol* 40(2):979–1006
- Nair MA, Kumar VS (2017) Wave spectral shapes in the coastal waters based on measured data off Karwar on the western coast of India. *Ocean Science* 13(3):365–378
- Nair MA, Kumar VS, George V (2021) Evolution of wave spectra during sea breeze and tropical cyclone. *Ocean Eng* 219:108341
- Nayak S, Bhaskaran PK, Venkatesan R, Dasgupta S (2013) Modulation of local wind-waves at Kalpakkam from remote forcing effects of Southern Ocean swells. *Ocean Eng* 64:23–35
- Neetu S, Shetye S, Chandramohan P (2006) Impact of sea breeze on wind-seas off Goa, west coast of India. *J Earth Syst Sci* 115(2):229–234
- Patra SK, Mishra P, Mohanty PK, Pradhan UK, Panda US, Murthy MR, Kumar VS, Nair TB (2016) Cyclone and monsoonal wave characteristics of northwestern Bay of Bengal: long-term observations and modeling. *Nat Hazards* 82(2):1051–1073
- Patra A, Bhaskaran PK, Maity R (2019) Spectral wave characteristics over the head Bay of Bengal: a modeling study. *Pure Appl Geophys* 176(12):5463–5486
- Sandhya KG, Nair TB, Bhaskaran PK, Sabique L, Arun N, Jeykumar K (2014) Wave forecasting system for operational use and its validation at coastal Puducherry, east coast of India. *Ocean Eng* 80:64–72
- Sanil Kumar V, Anjali Nair M (2015) Inter-annual variations in wave spectral characteristics at a location off the central west coast of India. In *Annales Geophysicae* 33(2):159–167
- Sanil Kumar V, Sajiv Philip C, Balakrishnan Nair TN (2010) Waves in shallow water off west coast of India during the onset of summer monsoon. In *Annales Geophysicae* 28(3):817–824
- Sanil Kumar V, Johnson G, Dubhashi KK, Nair B (2013) Waves off Puducherry, Bay of Bengal, during cyclone THANE. *Nat Hazards* 69(1):509–522
- Satish S, Sannasiraj SA, Sundar V (2019) Estimation and Analysis of Extreme Maximum Wave Heights. In *Proceedings of the Fourth International Conference in Ocean Engineering (ICOE2018)* Springer, Singapore 723–732.
- Semedo A, Sušelj K, Rutgersson A, Sterl A (2011) A global view on the wind sea and swell climate and variability from ERA-40. *J Climate* 24(5):1461–1479
- Simpson M, Warrior H, Raman S, Aswathanarayana PA, Mohanty UC, Suresh R (2007) Sea-breeze-initiated rainfall over the east coast of India during the Indian southwest monsoon. *Nat Hazards* 42(2):401–413
- Soares CG (1991) On the occurrence of double peaked wave spectra. *Ocean Eng* 18(1–2):167–171
- Sreelakshmi S, Bhaskaran PK (2020a) Wind-generated wave climate variability in the Indian Ocean using ERA-5 dataset. *Ocean Eng* 209:107486
- Sreelakshmi S, Bhaskaran PK (2020b) Regional wise characteristic study of significant wave height for the Indian Ocean. *Climate Dynam* 54(7):3405–3423
- Srinivas CV, Venkatesan R, Singh AB (2005) A numerical study of the influence of synoptic flow on coastal meso-scale circulations on the East and West coasts of India. *Mausam* 56(1):73–82
- Swain J, Umesh PA, Rao AD, Mishra SK (2017) Wave hindcast experiments using Wam Cycle 4.5. 3-Validation with in-situ measurements in the North Indian Ocean. *J Oceanogr Mar Res* 5(169):2
- Thompson WC, Nelson AR, Sedivy DG (1984) Wave group anatomy. In: *Proceedings of 19th Conference on Coastal Engineering Vol. I*. American Society of Civil Engineers, Houston Texas, pp 661–677
- Umesh PA, Swain J, Balchand AN (2018) Inter-comparison of WAM and WAVEWATCH-III in the North Indian Ocean using ERA-40 and QuikSCAT/NCEP blended winds. *Ocean Eng* 164:298–321
- Umesh PA, Bhaskaran PK, Sandhya KG, Nair TB (2019a) Spectral modelling on the characteristics of high frequency tail in shallow water wave spectra at Coastal Puducherry, East Coast of India. *Pure Appl Geophys* 176(1):501–524
- Umesh PA, Bhaskaran PK, Sandhya KG, Nair TB (2019b) Numerical simulation and preliminary analysis of spectral slope and tail characteristics using nested WAM-SWAN in a shallow water application off Visakhapatnam. *Ocean Eng* 173:268–283
- Umesh PA, Behera MR (2020) Performance evaluation of input-dissipation parameterizations in WAVEWATCH III and comparison of wave hindcast with nested WAVEWATCH III-SWAN in the Indian Seas. *Ocean Eng* 202:106959
- Vanem E, Walker SE (2013) Identifying trends in the ocean wave climate by time series analyses of significant wave height data. *Ocean Eng* 61:148–160
- Vethamony P, Aboobacker VM, Sudheesh K, Babu MT, Kumar KA (2009) Demarcation of inland vessels' limit off Mormugao port region, India: a pilot study for the safety of inland vessels using wave modelling. *Nat Hazards* 49(2):411–420
- Vimala J, Latha G, Venkatesan R (2014) Validation of in situ wave spectrum with JONSWAP in the Indian Ocean. *Int J Remote Sens* 35(14):5384–5393
- Young IR (2006) Directional spectra of hurricane wind waves. *J Geophys Res* 111(C8):C08020

Springer Nature or its licensor (e.g. a society or other partner) holds exclusive rights to this article under a publishing agreement with the author(s) or other rightsholder(s); author self-archiving of the accepted manuscript version of this article is solely governed by the terms of such publishing agreement and applicable law.